EFFECT OF RANDOM ANTENNA-POSITION ERRORS ON A LEAST-SQUARES DIRECT DATA DOMAIN APPROACH FOR SPACE-TIME ADAPTIVE PROCESSING

Seunghyeon Hwang and Tapan. K. Sarkar
Department of Electrical Engineering and Computer Science
3-114 Center for Science and Technology
Syracuse University
Syracuse, NY 13244-4100

Received 18 November 2004

ABSTRACT: *The equivalent isotropically radiated power (EIRP) degradation due to random position errors for space-time adaptive processing (STAP) is presented, based on the relationship between the EIRP degradation and the standard deviation or the uniform bound of the probability distribution of location of the antenna elements. We simulate a direct data domain least-squares (D^3LS) approach for STAP. In this simulation, two situations are considered. In the first case, the antenna elements at every time instance are assumed to have different spatial positions from the previous time instance. For the other case, the antennas are assumed to be randomly located, but are assumed to be fixed in a coherent processing interval (CPI). It is demonstrated that whether the locations of the antenna are fixed or vary within a CPI with identical random errors, the output signal-to-interference and noise ratio (SINR) are almost the same. When the antenna elements are moved randomly, the output SINR is less than the unperturbed case. We can develop a bound on the EIRP degradation due to the D^3LS approach to STAP based on the random position errors.* © 2005 Wiley Periodicals, Inc. Microwave Opt Technol Lett 45: 388–393, 2005; Published online in Wiley InterScience (www.interscience.wiley.com). DOI 10.1002/mop.20832

Key words: *random position; array antenna; space-time adaptive processing (STAP)*

1. INTRODUCTION

The direct data domain least-squares (D^3LS) approaches are based on the work of Sarkar and Sangruji [1]. Then Sarkar et al. [3, 4] presented two more variations to this approach, the backward processor and the forward-backward processor. These algorithms were then extended to the space-time domain; Park [5] described a generalized eigenvalue-based processor and Sarkar et al. [6] implemented the D^3LS processors.

The D^3LS STAP algorithm is used for suppressing highly dynamic clutter and interference. This enables the system to detect potentially weak target returns. In this analysis, we assume that the system consists of a linear array of N equally spaced antenna elements. We assume that the system processes a number of pulses (M) within a coherent processing interval (CPI). Each pulse repetition interval (PRI) consists of the transmission of a pulsed waveform of finite bandwidth and the reception of the reflected energy by the radar aperture and receivers, with a bandwidth matched to that of the radar pulse. Data can be arranged into a 3D matrix commonly referred to as a data cube [7]. We assume that the signals entering the array are narrowband, with a planar phase front, and consist of an SOI along with interference plus noise. The noise (thermal noise) originates in the receiver and is understood to be independent across elements and pulses. The interference is external to the receiver and consists of clutter, jammers, and signal multipath, which may be coherent or incoherent. For a uniformly spaced linear array (ULA), the complex envelope of the received SOI with unity amplitude, for the m^{th} pulse and n^{th} antenna element, can be described by

$$S_{m,n} = \exp\left[j2\pi\left\{\frac{(n-1)d}{\lambda}\cos(\phi_S) + \frac{(m-1)f_d}{f_r}\right\}\right], \quad \text{for } m = 1, 2, \ldots, M;\ n = 1, 2, \ldots, N, \tag{1}$$

where d is the inter-element spacing between the antenna elements, λ is the wavelength, f_r is the pulse repetition frequency, ϕ_S is the angle of arrival, and f_d is the Doppler frequency of the SOI. For the n^{th} antenna element and m^{th} pulse, the complex envelope of the received signal is given by

$$X_{m,n} = \alpha_S \cdot S_{m,n} + \text{Interference} + \text{Noise}, \tag{2}$$

where α_S is the complex amplitude of the SOI entering the array. For a particular row of Eq. (2), the column-to-column phase difference, due to the SOI, is given by

$$Z_1 = \exp\left[j2\pi\frac{d}{\lambda}\cos(\phi_S)\right]. \tag{3}$$

The row-to-row phase difference in a given column, due to the Doppler of the SOI, is given by

$$Z_2 = \exp\left(j2\pi\frac{f_d}{f_r}\right). \tag{4}$$

For the 2D case, these differences are performed with elements offset in space, time, and jointly in space and time. The three types of difference equations are then given by

$$X_{m,n} - Z_1^{-1} \cdot X_{m,n+1}, \tag{5}$$

$$X_{m,n} - Z_2^{-1} \cdot X_{m+1,n}, \tag{6}$$

$$X_{m,n} - Z_1^{-1} \cdot Z_2^{-1} \cdot X_{m+1,n+1}. \tag{7}$$

Now, we can form the cancellation rows in matrix $[F]$ using Eqs. (5)–(7), which will deal with only the undesired signals. And the elements of the first row of matrix $[F]$ is implemented as follows:

$$[1, Z_1, Z_1^2, \ldots, Z_1^{N_a-1}, \quad Z_2, Z_1Z_2, Z_1^2Z_2, \ldots Z_1^{N_a-1}Z_2, Z_2^2, Z_1Z_2^2, \ldots, Z_1^{N_a-1}Z_2^{N_t-1}], \tag{8}$$

where N_a is the spatial dimension and N_t is the temporal dimension of the window. N_a and N_t must satisfy the following equations:

$$N_a \le \frac{N+1}{2}, \tag{9}$$

$$N_t \le \frac{M+1}{2}. \tag{10}$$

The resulting matrix equation is then given by

$$[F][W] = [Y] = [C \quad 0 \quad \cdots \quad 0]^T. \tag{11}$$

The second process is to use the backward processor, which can be implemented by conjugating the element-pulse data and processing this data in reverse. We also use the forward-backward process, formed by combining the forward and backward solution procedure [3, 4].

When a D^3LS STAP is used, we assume that each antenna element is designated to be placed at a specific location [8]. In the real environment, however, it is possible for the location of the antenna elements to fluctuate due to an installation error or environmental effects. Research on random perturbations in the excitation coeffi-

TABLE 1 *x*, *y*, and *z*-Position Factors in the Expected Value Expression

Factor	Uniform Distribution	Gaussian Distribution
$\bar{H}_x$	$(\sin u\Delta_x/u\Delta_x)^2$	$e^{-u^2\sigma_x^2}$
$\bar{H}_y$	$(\sin v\Delta_y/v\Delta_y)^2$	$e^{-v^2\sigma_y^2}$
$\bar{H}_z$	$(\sin w\Delta_z/w\Delta_z)^2$	$e^{-w^2\sigma_z^2}$

cients of the antenna arrays has been the subject of several papers [9, 10]. These papers consider random perturbations of the amplitude and phase of the amplifiers. As a followup to the paper by Zaghloul [9] on the deteriation of the EIRP due to random perturbations in the excitation coefficients of the antenna array, in [12], Hwang and Sarkar presented allowable tolerances in the position of antenna elements for acceptable performance. In this paper, we identify how random position errors can affect a D^{3}LS approach when applied to STAP. Our goal is to determine how the system will perform when the antenna elements are randomly moved.

In section 2, we discuss EIRP degradation of the array antennas due to random-position errors in terms of the normalized EIRP degradation. In section 3, in order to explore the utility of the EIRP degradation, a probabilistic analysis of a simple phased-array antenna is studied. In section 4, the D^{3}LS approach for STAP are simulated using the relationship between the EIRP degradation and position errors due to random locations of the elements in an array.

2. EIRP DEGRADATION OF ARRAY ANTENNAS DUE TO RANDOM POSITION ERRORS

Consider an antenna array consisting of N antenna elements fed by N separate amplifiers. Except for a scaling factor, the far field $E(\theta, \phi)$ is given by

$$E(\theta, \phi) = \sum_{i=1}^{N} a_i e^{j(ux_i + vy_i + wz_i)} E_{el}(\theta, \phi), \tag{12}$$

where $a_i = |a_i| e^{j\psi_i}$ is the complex excitation coefficient for the i^{th} antenna element, x_i is the random perturbation of the x-coordinate of the i^{th} antenna element, y_i is the random perturbation of the y-coordinates of the i^{th} antenna element, z_i is the random perturbation of the z-coordinates of the i^{th} antenna element, $u = k \sin\theta \cos\phi$, $v = k \sin\theta \sin\phi$, $w = k \cos\theta$, $k = 2\pi/\lambda$, and $E_{el}(\theta, \phi)$ is the antenna-element pattern along the direction (θ, ϕ).

The probability-density functions of the random perturbations x_i, y_i, and z_i may be uniform or have Gaussian distributions. For uniform distributions, the probability density of x_i, y_i, and z_i are given by

$$p(x_i) = \frac{1}{2\Delta_x}, \quad \bar{x}_i - \Delta_x < x_i < \bar{x}_i + \Delta_x \tag{13}$$

$$= 0, \quad \text{otherwise},$$

$$p(y_i) = \frac{1}{2\Delta_y}, \quad \bar{y}_i - \Delta_y < y_i < \bar{y}_i + \Delta_y \tag{14}$$

$$= 0, \quad \text{otherwise},$$

$$p(z_i) = \frac{1}{2\Delta_z}, \quad \bar{z}_i - \Delta_z < z_i < \bar{z}_i + \Delta_z \tag{15}$$

$$= 0, \quad \text{otherwise}.$$

For Gaussian distributions, the probability-density functions for x_i, y_i, and z_i are given by

$$p(x_i) = \frac{1}{\sqrt{2\pi}\sigma_x} e^{-(x_i - \bar{x}_i)^2/2\sigma_x^2}, \tag{16}$$

$$p(y_i) = \frac{1}{\sqrt{2\pi}\sigma_y} e^{-(y_i - \bar{y}_i)^2/2\sigma_y^2}, \tag{17}$$

$$p(z_i) = \frac{1}{\sqrt{2\pi}\sigma_z} e^{-(z_i - \bar{z}_i)^2/2\sigma_z^2}, \tag{18}$$

where $\bar{x}_i$, $\bar{y}_i$, and $\bar{z}_i$ are the mean values of the x_i, y_i, and z_i positions, respectively, and σ_x^2, σ_y^2, and σ_z^2 are the variance of the x, y, and z coordinates, respectively.

According to Zaghloul [9], EIRP along the direction (θ, ϕ) is proportional to the power radiated in the same direction. Therefore EIRP, is given by

$$P = \sum_{i=1}^{N} |G_i|^2 + \sum_{\substack{i=1 \\ i \neq j}}^{N} \sum_{j=1}^{N} e^{j[u(x_i - x_j) + v(y_i - y_j) + w(z_i - z_j)]} G_i G_j^* \tag{19}$$

in which * denotes the complex conjugate, and

$$G_i = a_i \cdot E_{el}(\theta, \phi). \tag{20}$$

The probability distribution of the EIRP will be Gaussian with the mean of $\bar{P}$ and a standard deviation of $\sigma(P)$, based on the central-limit theory [11]. The probability distribution of the EIRP is within the confidence interval $[\bar{P} - n\sigma(P)]/P_0$, $[\bar{P} + n\sigma(P)]/P_0$. The left side of the confidence interval in the probability distribution of the EIRP, $[\bar{P} - n\sigma(P)]/P_0$, represents the worst case for all possible cases. Normalizing $\bar{P}$ and $\sigma(P)$ with respect to the unperturbed power P_0 presents the degradation in the EIRP of the array. This quantity, $[\bar{P} - n\sigma(P)]/P_0$, is the normalized

TABLE 2 *x*-, *y*-, and *z*-Position Factors in the Variance Expression

Factor	Uniform Distribution	Gaussian Distribution
$H_{1,x}$	$\left(\frac{\sin u\Delta_x}{u\Delta_x}\right)^2$	$e^{-u^2\sigma_x^2}$
$H_{1,y}$	$\left(\frac{\sin v\Delta_y}{v\Delta_y}\right)^2$	$e^{-v^2\sigma_y^2}$
$H_{1,z}$	$\left(\frac{\sin w\Delta_z}{w\Delta_z}\right)^2$	$e^{-w^2\sigma_z^2}$
$H_{2,x}$	$\left(\frac{\sin 2u\Delta_x}{2u\Delta_x}\right)^2$	$e^{-4u^2\sigma_x^2}$
$H_{2,y}$	$\left(\frac{\sin 2v\Delta_y}{2v\Delta_y}\right)^2$	$e^{-4v^2\sigma_y^2}$
$H_{2,z}$	$\left(\frac{\sin 2w\Delta_z}{2w\Delta_z}\right)^2$	$e^{-4w^2\sigma_z^2}$
$H_{3,x}$	$\left(\frac{\sin u\Delta_x}{u\Delta_x}\right)^2\left(\frac{\sin 2u\Delta_x}{2u\Delta_x}\right)$	$e^{-3u^2\sigma_x^2}$
$H_{3,y}$	$\left(\frac{\sin v\Delta_y}{v\Delta_y}\right)^2\left(\frac{\sin 2v\Delta_y}{2v\Delta_y}\right)$	$e^{-3v^2\sigma_y^2}$
$H_{3,z}$	$\left(\frac{\sin w\Delta_z}{w\Delta_z}\right)^2\left(\frac{\sin 2w\Delta_z}{2w\Delta_z}\right)$	$e^{-3w^2\sigma_z^2}$
$H_{4,x}$	$\left(\frac{\sin u\Delta_x}{u\Delta_x}\right)^4$	$e^{-2u^2\sigma_x^2}$
$H_{4,y}$	$\left(\frac{\sin v\Delta_y}{v\Delta_y}\right)^4$	$e^{-2v^2\sigma_y^2}$
$H_{4,z}$	$\left(\frac{\sin w\Delta_z}{w\Delta_z}\right)^4$	$e^{-2w^2\sigma_z^2}$

EIRP degradation. Along the same line of the amplitude and phase perturbation in [9], we choose $n = 3$ so that the worst-case degradation of the EIRP is within 99.7% of all possible cases for the given random position distributions.

The expected value $\bar{P}$ and the standard deviation $\sigma(P)$ of P can be expressed in separable terms containing the statistical parameters for x_i, y_i, and z_i. Each amplifier is located at each x, y, and z position and is considered to be independent. They have the same distribution. An expression for the influence of random locations of the antenna elements can be calculated by integrating the product of the probability distribution and the power P. The expected value $\bar{P}$ is obtained as

$$\bar{P} = \sum_{i=1}^{N} |G_i|^2 + \bar{H}_x \bar{H}_y \bar{H}_z \sum_{i=1}^{N} \sum_{j=1}^{N} e^{j[u(\bar{x}_i - \bar{x}_j) + v(\bar{y}_i - \bar{y}_j) + w(\bar{z}_i - \bar{z}_j)]} G_i G_j^*, \tag{21}$$

where $\bar{H}_x$ is the x-position variation-dependent factor, $\bar{H}_y$ is the y-position variation-dependent factor, and $\bar{H}_z$ is the z-position variation-dependent factor. These expressions are given in Table 1.

The next step in calculating the standard deviation $\sigma(P)$ indicates the extent of the array EIRP degradation. The standard deviation is given by

$$\sigma(P) = \sqrt{\text{var}(P)} \tag{22}$$

and the variance is defined as

$$\text{var}(P) = E[P^2] - \bar{P}^2, \tag{23}$$

in which $E[\cdot]$ denotes the expectation value. We obtain $E[P^2]$ as follows:

$$\begin{aligned} E[P^2] = {} & \sum_{i=1}^{N} |G_i|^4 + 2 \times \sum_{\substack{i=1 \\ i \neq j}}^{N} \sum_{j=1}^{N} |G_i|^2 |G_j|^2 + 4 \times H_{1,x} H_{1,y} H_{1,z} \sum_{\substack{i=1 \\ i \neq j}}^{N} \sum_{j=1}^{N} e^{j[u(\bar{x}_i - \bar{x}_j) + v(\bar{y}_i - \bar{y}_j) + w(\bar{z}_i - \bar{z}_j)]} |G_i|^2 G_i G_j^* + 4 \\ & \times H_{1,x} H_{1,y} H_{1,z} \sum_{\substack{k=1 \\ k \neq i \neq j}}^{N} \sum_{i=1}^{N} \sum_{j=1}^{N} e^{j[u(\bar{x}_i - \bar{x}_j) + v(\bar{y}_i - \bar{y}_j) + w(\bar{z}_i - \bar{z}_j)]} |G_k|^2 G_i G_j^* + H_{2,x} H_{2,y} H_{2,z} \sum_{\substack{i=1 \\ i \neq j}}^{N} \sum_{j=1}^{N} e^{j2[u(\bar{x}_i - \bar{x}_j) + v(\bar{y}_i - \bar{y}_j) + w(\bar{z}_i - \bar{z}_j)]} G_i^2 G_j^{*2} \\ & + H_{3,x} H_{3,y} H_{3,z} \sum_{\substack{k=1 \\ k \neq i \neq j}}^{N} \sum_{i=1}^{N} \sum_{j=1}^{N} [e^{j[u(\bar{x}_k + \bar{x}_i - 2\bar{x}_j) + v(\bar{y}_k + \bar{y}_i - 2\bar{y}_j) + w(\bar{z}_k + \bar{z}_i - 2\bar{z}_j)]} G_k G_i G_j^{*2} + e^{j[u(-\bar{x}_k + 2\bar{x}_i - \bar{x}_j) + v(-\bar{y}_k + 2\bar{y}_i - \bar{y}_j) + w(-\bar{z}_k + 2\bar{z}_i - \bar{z}_j)]} G_k G_i^2 G_j^*] \\ & + H_{4,x} H_{4,y} H_{4,z} \sum_{\substack{k=1 \\ k \neq l \neq i \neq j}}^{N} \sum_{l=1}^{N} \sum_{i=1}^{N} \sum_{j=1}^{N} e^{j[u(\bar{x}_k - \bar{x}_l + \bar{x}_i - \bar{x}_j) + v(\bar{y}_k - \bar{y}_l + \bar{y}_i - \bar{y}_j) + w(\bar{z}_k - \bar{z}_l + \bar{z}_i - \bar{z}_j)]} G_k G_l^* G_i G_j^*, \end{aligned} \tag{24}$$

where the factors $H_{*,x}$, $H_{*,y}$, and $H_{*,z}$ result from estimating constituents of the second moment of the power P, and are given in Table 2 for the uniform and Gaussian distributions.

3. EXAMPLE OF EIRP DEGRADATION IN ANTENNA ARRAYS

To explore the utility of the EIRP degradation, a probabilistic analysis on a simple linear phased array antenna is performed, as shown in Figure 1. Using this example, we investigate how the EIRP degradation behaves as a function of the various parameters.

Consider a linear array consisting of 10 elements (Fig. 1). The array consists of 10 isotropic omnidirectional point radiators and is fed by 10 amplifiers. The elements of the linear array are equally spaced and their inter-element spacing along the x direction is given by 0.4775λ ($\lambda = 1$ m). To simplify the example, we assume that all the elements are located at $z = 0$, so that the z positions of all the elements are fixed. Therefore the EIRP degradation of the linear array is caused by random perturbations in the x and y positions, which can have two types of probability distribution, either uniform or Gaussian. $\bar{H}_z$ is 1 according to the expected value of Eq. (21) and $H_{*,z}$ is also 1 in the 2nd moment of the power of Eq. (24). When the positions of all the elements are unperturbed, $\bar{H}_x$ and $\bar{H}_y$ equal unity, and also $\bar{P}$ becomes the unperturbed power P_0. As expected, the variance is identically zero, as given by Eq. (23).

The expected value and standard deviation are applied to the linear-array case in order to obtain the normalized EIRP degradation with $n = 3$ and $[\bar{P} - 3\sigma(P)]/P_0$. Of special interest is the EIRP degradation within the half-power beam width between $\phi = 90°$ and $\phi = 95.33°$. Figures 2 and 3 show the worst case degradation with $3\sigma(P)$. Figure 2 represents the case for the Gaussian perturbation with $\sigma_{x \text{ and } y} = 0.0$, 0.03, 0.05, and 0.07 [m], and Figure 3 represents uniform perturbation with $\Delta_{x \text{ and } y} = 0.0$, 0.03, 0.05, and 0.07 [m]. As expected, the unperturbed case shows a 0-dB value for all the angles. The EIRP degrades with the larger standard deviation of the Gaussian perturbation and the uniform bounds for a uniform perturbation. The EIRP due to the random positions of the antennas is significantly decreased.

The normalized EIRP degradation, $[\bar{P} - 3\sigma(P)]/P_0$, represents the worst case for 99.7 percent of all possible cases, as mentioned previously. This value, however, depends on different values of σ for a Gaussian distribution or has a different Δ for a uniform distribution, as can be seen from Figures 2 and 3. The question is what is the allowable tolerance for σ and Δ and for the elements to operate appropriately in the antenna system for adaptive signal processing.

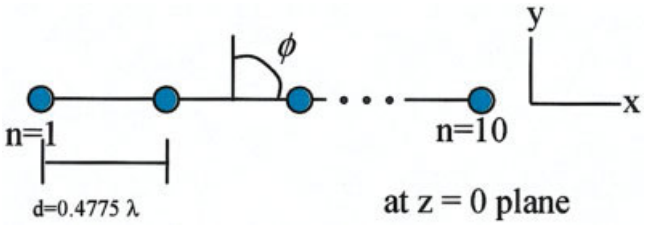

Figure 1 Uniformly spaced linear-array configuration. [Color figure can be viewed in the online issue, which is available at www.interscience.wiley.com.]

We focus on the main lobe, especially inside the half-power beam width. To choose the appropriate values of $\sigma_{x \text{ and } y}$ and $\Delta_{x \text{ and } y}$, we select the point that makes the 3-dB loss below the optimum for the normalized EIRP degradation graph, at the angle corresponding to the half-power beam width. At this −3-dB point, the antenna performance using conventional beam forming will be significantly decreased. However, the 3-dB loss of the normalized EIRP degradation at the angle of the half-power beam is the allowable worst case for an antenna system to operate properly, compared to the unperturbed case. From these values of σ and Δ, obtained from the 3-dB loss point of the normalized EIRP degradation, we investigate how the system behaves if the antenna elements are randomly perturbed by those σ and Δ.

As illustrated in Figure 4, the −3-dB point of the normalized EIRP degradation with $n = 3$ of a uniform linear array occurs at 95.33° with $\sigma_{x \text{ and } y} = 0.042$ m and $\Delta_{x \text{ and } y} = 0.072$ m. Figure 4 also illustrates that the relationship between the normalized EIRP degradation with $n = 3$ and $\sigma_{x \text{ and } y}$, and between the normalized EIRP degradation and $\Delta_{x \text{ and } y}$ at a specific angle, 95.33°. The larger the $\sigma_{x \text{ and } y}$ and $\Delta_{x \text{ and } y}$, the lower the normalized EIRP degradation. We apply these values, $\sigma_{x \text{ and } y} = 0.042$ m and $\Delta_{x \text{ and } y} = 0.072$ m, and then investigate how the random position errors affect the D^{3}LS approach for STAP.

4. SIMULATION RESULTS

The received signals modeled in this simulation consist of the SOI, main-beam clutter, discrete interferers, jammers, and thermal noise. The clutter is modeled as point scatterers placed approximately every 0.1° apart. The amplitude of the clutter points are modeled with a normal distribution about a mean that results in a signal-to-clutter ratio (SCR) of −12.7 dB. Ten strong point scatterers are modeled in this simulation, based on the angle of arrival (AOA) and Doppler parameters, as defined in Table 3. Each example of thermal noise generated in each receive channel is independent from the others. The resulting SNR is approximately 30 dB. The jammer is modeled as a broadband noise signal that arrives from 100° in azimuth, and covers all Doppler frequencies of interest. Summing the power of the interfering sources received by the first channel and comparing it to the power of the SOI, the average input signal-to-interference plus noise ratio (SINR) is evaluated as −18.6 dB. And random-position errors of the antenna element are $\sigma_{x \text{ and } y} = 0.042$ m and $\Delta_{x \text{ and } y} = 0.072$ m. While

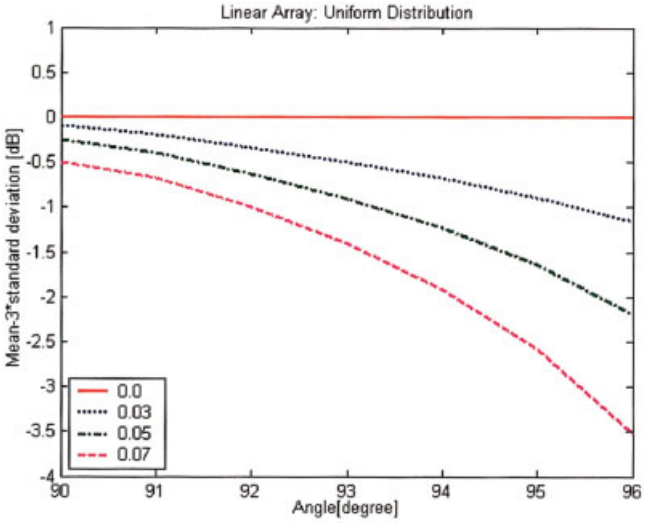

Figure 3 Normalized EIRP degradation with $n = 3$ for uniform perturbation with different bounds of $\Delta_{x \text{ and } y} = 0.0$, 0.03, 0.05, and 0.07 [m]. [Color figure can be viewed in the online issue, which is available at www.interscience.wiley.com.]

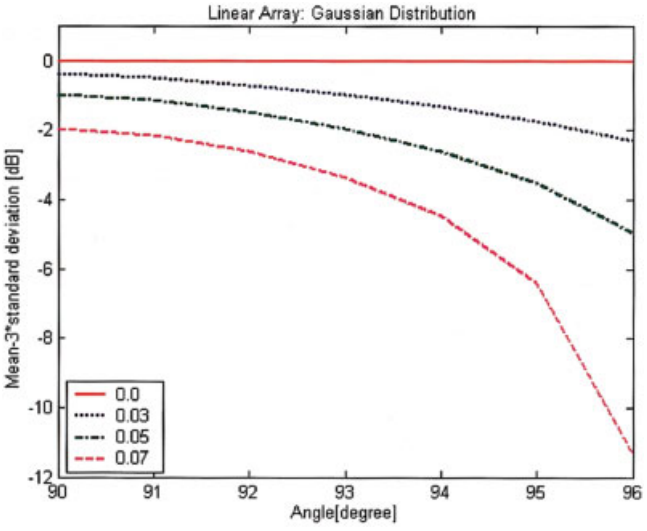

Figure 2 Normalized EIRP degradation with $n = 3$ for Gaussian perturbation with standard deviation of $\sigma_{x \text{ and } y} = 0.0$, 0.03, 0.05, and 0.07 [m]. [Color figure can be viewed in the online issue, which is available at www.interscience.wiley.com.]

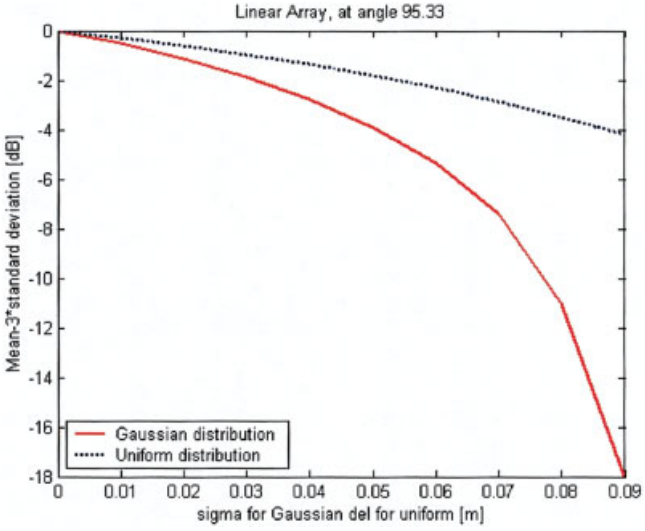

Figure 4 The relationship between the normalized EIRP degradation with $n = 3$, and $\sigma_{x \text{ and } y}$ and $\Delta_{x \text{ and } y}$ at the angle 95.33° for a linear array. [Color figure can be viewed in the online issue, which is available at www.interscience.wiley.com.]

TABLE 3 Parameters Related to the Simulation

Wavelength		1 m	Signal	AOA	60°
Pulse Rep. Freq		4 kHz		Doppler	1169 Hz
Number of Antennas		$N = 10$		SNR	30 dB
Number of Pulses		$M = 16$	Jammer	AOA	100°
Half-Power Beamwidth		10.66°		Doppler	Covers all Doppler frequencies of interest
Processor	Forward	$N_a = 7$, $N_t = 9$	Discrete interferes	AOA	[85° 120° 40° 35° 30° 140° 100° 70° 50° 125°]
	Forward-Backward	$N_a = 8$, $N_t = 9$			
Clutter	Extent	Main beam		Doppler	[400 −800 1700 −1400 325 −1650 950 −1200 −125 1450] Hz
	Point scatterers	0.1° apart in angle			

processing the signal, the antenna elements are randomly moved. In this simulation, we consider two situations: one in which the antenna elements at every time instance have different spatial positions from the previous time instance, and another in which the antenna's random locations are fixed within a CPI.

With $N = 10$ channels and $M = 16$ pulses, the performance of the three D^{3}LS algorithms (namely, the forward, backward, and the forward and backward methods) is evaluated based on the weights and the output SINR. The forward and backward methods utilize seven spatial (N_a) and nine temporal (N_t) degrees of freedom (DOF), resulting in a total of 63 DOF, while the forward-backward method employs eight spatial and nine temporal DOF, for a total of 72 DOF. The spectrum of the input signal is shown in Figure 5. Here, the circles indicate the locations of the discrete interferers and the triangles define the location of the main beam clutter and the + symbol indicates the location of the SOI.

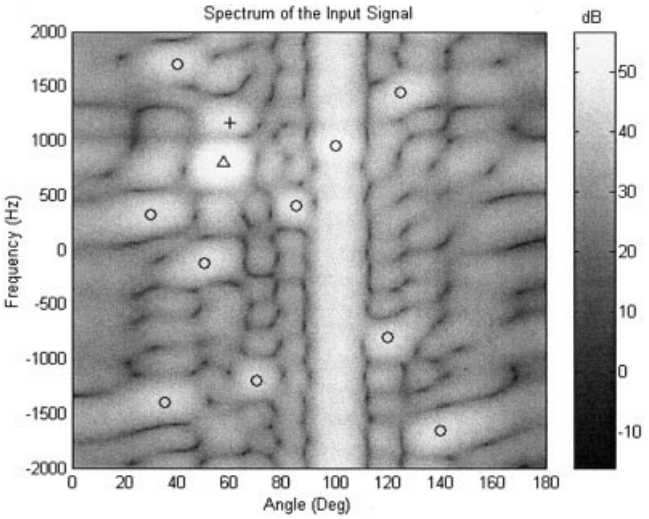

Figure 5 Spectrum of the input signal

Table 4 shows the output SINR for the unperturbed case, the perturbed case with a Gaussian profile, and a uniform profile. These values are averaged over 100 runs. The resulting weights for the unperturbed case and for the perturbed case with Gaussian and uniform density functions using the forward method are shown in Figures 6–8, when the antenna elements at every time instance have different spatial positions from the previous time instance. The antenna positions are randomly located with $\sigma_{x \text{ and } y} = 0.042$ m or $\Delta_{x \text{ and } y} = 0.072$ m. The output SINR of the Gaussian and uniform perturbed cases are lower than the output SINR of the unperturbed case. Even though we choose different values of σ and Δ, we obtain approximately an output SINR of ± 11 dB. This shows that we realize EIRP degradation which can be obtained analytically. From Figures 7 and 8, the system with random positions generates nulls that are slightly moved from the angle of arrival (AOA) of discrete interferers, as compared to the unperturbed case. The output SINR of the unperturbed case is about 18–19 dB, and the output SINRs for the Gaussian and uniform density distributions are about 11 dB when the antenna elements at every time instance have different spatial positions from the previous time instance. This perturbed system still removes the jammer, clutters, discrete interferers, and noise. When the random locations of the antenna are fixed in a CPI, one also obtains almost the same output SINR. The value of the output is dependent on the value of the tolerance of the antenna elements.

From these results, as long the antenna element position errors are within the limits set by $\sigma = 0.042$ m for the Gaussian distribution and $\Delta = 0.072$ m for the uniform distribution, the adaptive array has a reasonable performance for STAP. If we want to provide stricter tolerances in the distribution of the antenna elements, that is, $\sigma < 0.042$ m for the Gaussian distribution and $\Delta < 0.072$ m for the uniform distribution, then one can obtain higher output SINR, which may be close to the output SINR for the

TABLE 4 Output-Signal-to-Interference Plus Noise Ratio

		Case A (The Antenna's Random Locations are Changed Every Time Instance)	Case B (The Antenna's Random Locations are Fixed in a CPI)
Forward	Unperturbed	18.210 [dB]	
	Gaussian	11.458[dB]	11.028[dB]
	Uniform	11.480[dB]	10.515[dB]
Backward	Unperturbed	18.210 [dB]	
	Gaussian	11.458[dB]	11.028[dB]
	Uniform	11.480[dB]	10.515[dB]
Forward-Backward	Unperturbed	19.213 [dB]	
	Gaussian	11.481[dB]	11.150[dB]
	Uniform	11.844[dB]	11.183[dB]

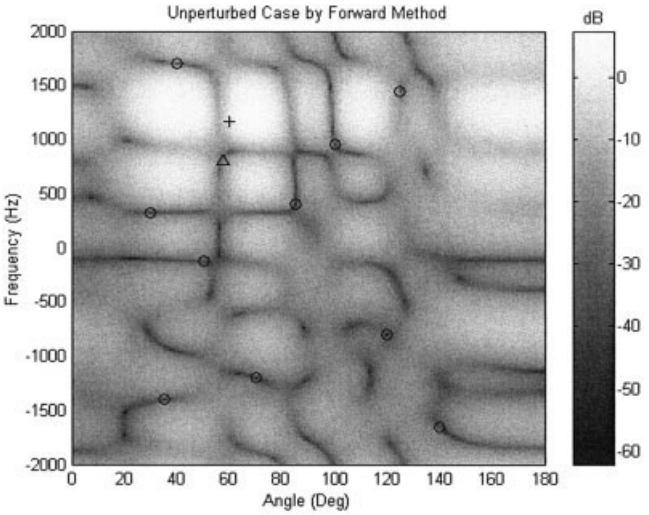

Figure 6 Forward-method weight spectrum for the unperturbed case

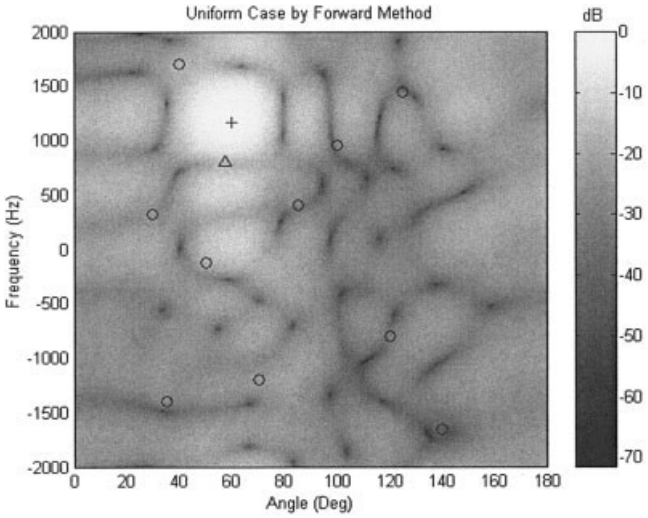

Figure 8 Forward-method weights for the perturbed uniform profile with $\Delta_{x \text{ and } y} = 0.072$ m

unperturbed case. As a result, one can predict how much the system would be degraded by analytically solving the problem using the normalized EIRP degradation.

5. CONCLUSION

In this paper, expressions have been derived for the expected value, standard deviation, and normalized EIRP degradation with $n = 3$ due to the random locations of the array elements. The normalized EIRP degradation represents the worst case for 99.7% of all possible cases. We have investigated the effects of random antenna positions using a D^{3}LS approach for STAP for these EIRP degradations, according to the random position of the array elements. Even though $\sigma = 0.042$ m for the Gaussian distribution and $\Delta = 0.072$ m for the uniform distribution are given for the antenna elements, we can still obtain an acceptable output SINR. When the antenna elements at every time instance have different spatial positions from the previous time instance, the output SINR is almost the same as in the case where the antenna elements are located at fixed random locations within a CPI. In this paper, the results for the EIRP degradation have been predicted for the Gaussian and the uniform perturbed cases. Random antenna-position errors degrade the output SINR of the D^{3}LS approach for STAP.

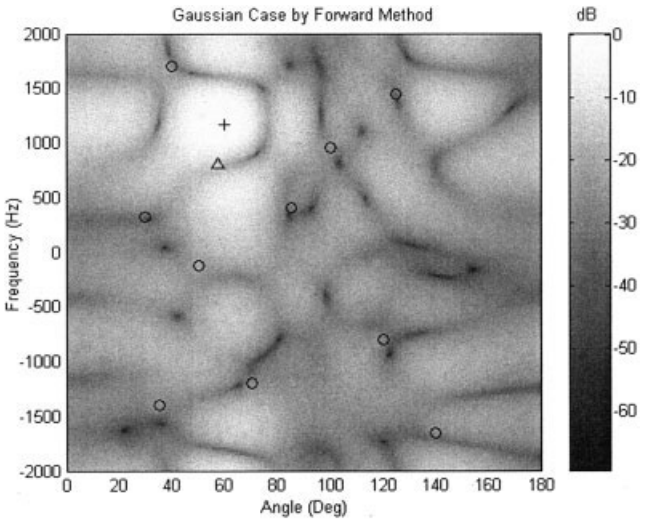

Figure 7 Forward-method weights for the perturbed Gaussian profile with $\sigma_{x \text{ and } y} = 0.042$ m

REFERENCES

1. T.K. Sarkar and N. Sangruji, An adaptive nulling system for a narrowband signal with a look direction constraint utilizing the conjugate-gradient method, IEEE Trans Antennas Propagat 37 (1989), 940–944.
2. R. Schneible, A least square approach for radar array adaptive nulling, doctoral dissertation, Syracuse University, 1996.
3. T.K. Sarkar, J. Koh, R. Adve, R. Schneible, M. Wicks, S. Choi, and M. Salazar-Palma, A pragmatic approach to adaptive antennas, IEEE Antennas Propagat Mag 42 (2000), 39–55.
4. T.K. Sarkar, S. Park, J. Koh, and R.A. Schneible, A deterministic least-squares approach to adaptive antennas, Digital Signal Processing Rev J 6 (1996), 185–194.
5. S. Park, Estimation of space-time parameters in nonhomogeneous environment, doctoral dissertation, Syracuse University, 1996.
6. T.K. Sarkar, H. Wang, S. Park, J. Koh, R. Adve, K. Kim, Y. Zhang, M.C. Wicks, and R.D. Brown, A deterministic least-square approach to space-time adaptive processing (STAP), IEEE Trans Antennas Propagat 49 (2001), 91–103.
7. J.T. Carlo, T.K. Sarkar, and M.C. Wicks, A least-squares multiple constraint direct data domain approach for STAP, IEEE Radar Conf Proc 2003, pp. 431–438.
8. T.K. Sarkar, M.C. Wicks, M. Salazar-Palma, and R.J. Bonneau, Smart antennas, Wiley–IEEE Press, Hoboken and Piscataway, NJ, 2003.
9. A.I. Zaghloul, Statistical analysis of EIRP degradation in antenna arrays, IEEE Trans Antennas Propagat AP-33 (1985), 217–221.
10. P. Snoeij and A.R. Vellekoop, A statistical model for the error bounds of an active phased array antenna for SAR applications, IEEE Trans Geosci Remote Sensing 30 (1992), 736–742.
11. A. Papoulis, Probability, random variables, and stochastic processes, 3rd ed., McGraw-Hill, New York, 1991.
12. S. Hwang and T.K. Sarkar, Allowable tolerances in the position of antenna elements in an array amenable to adaptive processing, Microwave Opt Technol Lett 43 (2004), 215–221.